ISSN 1727-7337 (print)
ISSN 2663-2217 (online)

UDC 629.7.036.73: 533.933

doi: 10.32620/aktt.2026.4.05

Shahram ROSHANPOUR

IL Sentiero International Campus, Schio VI, Italy

THE ANALYSIS OF THE MUTUAL DEPENDENCE OF IMPACT IONIZATION AND ELECTRON ENERGY DISTRIBUTION IN ELECTRIC PROPULSION DEVICES

*The **object** of this study is the set of physical processes in the non-equilibrium plasma of electric propulsion devices. The **subject** of the study is impact ionization, specifically the feedback effect on the electron energy spectrum. The **aim** of the study is to derive expressions for the impact ionization characteristics in the right-hand sides of the mathematical model equations describing electric propulsion devices based on the compromise kinetic-fluid model. The **objectives** of the study are: to analyze existing continuum mechanics models that incorporate the impact ionization process building upon the results presented in the author's previous works; to write an expression for the average values over the electron energy spectrum of the ionization volume coefficient and cross-section and to analyze the behavior of the calculated values taking into account the interdependence of ionization processes and the formation of the electron energy distribution. **The methods** used in the study include an analytical investigation of existing process models to determine their limits of applicability in rarefied plasma, as well as a theoretical analysis of the impact of ionization on the electron energy spectrum, taking into account the characteristics of plasma confined by potential barriers in a boundary bipolar layer. Calculated energy-dependent distributions above the potential barrier yielded lower values than those obtained for a Maxwellian distribution; however, higher values were observed below the ionization potential at elevated electron temperatures. Based on an analysis of the influence of the electron energy spectrum on the ionization intensity and the influence of the electromagnetic field on electron transport in energy space, a positive feedback was demonstrated: at relatively high electron temperatures, the need to transport them "upward" from the region below the ionization potential leads to an excess of electrons in this region. In turn, this surplus increases the energy-averaged ionization cross-section, further reinforcing the electron excess in the lower energy spectrum.*

Keywords: *electric propulsion devices, electrons energy distribution; impact ionization; potential barrier; bipolar boundary layer; angular moments model.*

1. Introduction

1.1. Motivation

Electric propulsion devices (EPD) include electric thermal thrusters, plasma-ion thrusters, Hall thrusters, helicon thrusters, as well as plasma, ion, and electron sources. With the exception of electric thermal thrusters, one of the most important processes in these devices, responsible for their operation and performance characteristics, is the impact ionization of the propellant atoms.

The quantitative characteristics of impact ionization depend on the electron energy distribution. The electron energy spectrum, in turn, is determined by a series of processes, one of which is ionization.

1.2. State of the art

The most accurate mathematical model of EPD processes is the system of kinetic equations [1]. However, using this model requires calculating the distributions of at least three components (atoms, ions, and electrons) as functions of time, three coordinate projections, and three velocity projections.

The next as for accuracy is the electric gas dynamics (EGD) system [2] within the local thermodynamic equilibrium (LTE) method. However, the dissipative components of the momentum (viscosity) and energy (thermal conductivity) flux densities are only applicable to dense gases, where these characteristics change little over time and the mean free path, which is inconsistent with the EPD conditions.

Two approaches that emerged at the end of the 20th century are an attempt to solve this problem.

The first approach is presented in a series of publications as the Hybrid PIC-Fluid (HPICFlu) model [3]:

- Electron dynamics is described by EGD tools within the LTE framework under the assumption of a Maxwell distribution of electrons velocity [4], which is again possible in sufficiently dense gases and is not realized in the rarefied plasma of EPD.

- In the PIC section of [5, 6], the problem is solved by dividing the thruster volume into 20-30 cells in each of two directions, with an average of 30 so-called macro-particles in each cell. It can be shown that this number of macro-particles results in a relative standard error of approximately 18%. In the cited work, this manifested itself in a violation of the mass law of conservation in the distribution of atomic and ion flows, as well as a discrepancy between the calculated and measured ion currents, not only in magnitude but also in direction, over almost half the channel length.

The second approach is presented in a series of publications called Angular moments models for rarefied gas dynamics (AMM) [7], using parameters and equations in a form intermediate between kinetics and EGD. The main problem in this series is the limitations of the existing traditional notation, which does not allow for the use of universal notations for tensors of arbitrary ranks:

- This led to a limitation of the system of equations, which are angular analogues of continuity and motion equations in EGD. The authors of [8] announce AMM as a more accurate model compared to LTE. The method of closing the equations system, based on the so-called "entropy minimization principles" procedure, leads to a recording of the electron velocity distribution, which is an implicit form of the Maxwell distribution, and the approximation error, relating the second-rank tensor to a scalar and a vector, becomes less than 10% only for hypersonic electron flow, which is not typical for EPD.

Unlike LTE, the resulting system of equations does not contain viscosity and thermal conductivity even approximately. In [9], a comparison of the results of solving a one-dimensional problem using the Navier-Stokes equation and the AMM method is presented. The “good” agreement between the results shown there is easily explained by the fact that, the Navier-Stokes equation gives zero values of the off-diagonal components of the viscosity tensor within the framework of a one-dimensional problem, while the AMM method always does.

- The mentioned limitation in the symbolism in the work [10] was also reflected in the violation of the momentum conservation law in electron-electron collisions.

Common feature in the shown works devoted to HPICFLU and AMM methods is the absence of records for ionization collisions and slightest attempt of analyze the electrons velocity distribution function.

The optimal method for modeling processes in EPD at the National Aerospace University "Kharkiv Aviation Institute", of which the author of this study is a graduate, is an approach that involves:

- solution of the EGD equations system using universal symbolism, which allows not to limit the rank of tensor parameters;

- finding some coefficients in the left-hand sides and collision terms in the right-hand sides of the EGD equations using kinetics or the methods of developed by us Compromise kinetic-fluid model (CKFM) [11].

1.3. Objectives and tasks

Taking into account the above, the aim of the study is to find expressions for the characteristics of impact ionization in the right-hand sides of the equations of the mathematical model of processes in EPD based on CKFM.

To achieve this goal, it is advisable to solve the following problems:

1. To analyze the sequence "kinetics – EGD – CKFM" taking into account the impact ionization process using the unified symbolism presented in the work [12].
2. To write down the expression for the average over the electron energy spectrum values of the volume coefficient and ionization cross-section.
3. To analyze the behavior of the calculated values taking into account the interdependence of ionization processes and the formation of electron energy distribution.

2. Materials and methods of research

The following scientific methods were used in the study:

- analytical method when studying of existing models of processes in EPD, with the determination of limits of their applicability in the rarefied plasma;

- theoretical methods at the analysis of a role of impact ionization in formation of electrons energy spectrum in view of features of plasma, limited by potential barriers in a boundary bipolar layer.

The object of the study is the processes in non-equilibrium plasma EPD.

The subject of the study is impact ionization, taking into account its feedback with the energy spectrum of electrons.

2.1. The sequence "kinetics – EGD – CKFM" as varieties of continuum mechanics

The most accurate approach within the framework of continuum mechanics is kinetics, the main tool of which is the particle velocity distribution function $f\left(t,\vec{r},\vec{v}\right)$ – the number of particles in 6-dimensional unit volume of coordinate-velocity space [1].

Tool for finding $f\left(t,\vec{r},\vec{v}\right)$ is a kinetic equation, the entry for which for electrons has the following form:

$$\frac{\partial f_e}{\partial t}+\nabla\cdot\left(f_e\vec{v}\right)-\frac{e}{m_e}\nabla_v\cdot\left(f_e\left(\vec{E}+\vec{v}\times\vec{B}\right)\right)=\frac{\delta f_e}{\delta t}, \qquad (1)$$

where e, m_e – elementary charge and mass of an electron; $\vec{E}$ and $\vec{B}$ – electric field strength and magnetic induction; $\nabla_v \cdot \vec{A}(\vec{v})$ – divergence of the vector in velocity space; $\frac{\delta f_e}{\delta t}$ – collision integral: change f_e per unit of time as a result of collisions in the volume.

The collision integral must, at a minimum, take into account electron-electron, electron-atom, electron-ion elastic collisions and ionization collisions:

$$\frac{\delta f_e}{\delta t} = \frac{\delta_{ee} f_e}{\delta t} + \frac{\delta_{ea} f_e}{\delta t} + \frac{\delta_{ei} f_e}{\delta t} + \frac{\delta_i f_e}{\delta t}, \qquad (2)$$

In this case, the recording of the integral of ionization collisions must take into account the transport of electrons from the region above to the region below the allocated volume in velocity space:

$$\frac{\delta_i f_e(\vec{v})}{\delta t} = \frac{\delta_e^- f_e(\vec{v})}{\delta t} + \frac{\delta_e^+ f_e(\vec{v})}{\delta t}, \qquad (3)$$

$$\frac{\delta_e^- f_e(\vec{v})}{\delta t} = -f_e(\vec{v}) v \sigma_i(v), \qquad (4)$$

$$\frac{\delta_e^+ f_e(\vec{v})}{\delta t} = \int\limits_{v' \ge \sqrt{v^2 + v_i^2}} f_e(\vec{v}') v' \sigma_i(v') p(\vec{v}', \vec{v}) d^3 v', \qquad (5)$$

$$m_e v_i^2 = 2 e \varphi_i, \qquad (6)$$

where σ_i – ionization cross-section; $p(\vec{v}', \vec{v})$ – the probability density of detecting a secondary electron with a velocity $\vec{v}$ as a result of ionization by a primary electron at a speed $\vec{v}'$; φ_i – ionization potential.

Any gas-dynamic parameter is a distribution function moment of a certain order – a tensor of the corresponding rank:

$$\mathbf{M}_e^{[k]}(t, \vec{r}) = m_e \int\limits_0^\infty \int\limits_\Omega f_e(t, \vec{r}, \vec{v}) \vec{v}^{\lceil k \rceil} v^2 dv\, d\Omega, \qquad (7)$$

where k – order of moment; Ω – solid angle in the spherical velocity reference system; $\vec{v}^{\lceil k \rceil} = \underbrace{\vec{v}\,\vec{v}\,\vec{v} \ldots \vec{v}}_{k \text{ tines}}$ – iteration [12] (factor [2]) of velocity.

Here $\mathbf{M}_e^{[0]} = \rho_M$ – mass density; $\mathbf{M}_e^{[1]} = \vec{p}^{(V)}$ – mass flux density ≡ momentum density; $\mathbf{M}_e^{[2]} = \mathbf{\Pi}$ – the momentum flux density, half of which trace is the energy density $\frac{1}{2} \mathrm{Tr}\, \mathbf{\Pi} = \varepsilon^{(V)}$; $\mathbf{M}_e^{[3]} = \mathbf{Q}$ – an unnamed 3rd rank tensor, half of which trace is the energy flux density $\frac{1}{2} \mathrm{Tr}\, \mathbf{Q} = \vec{q}$.

Using the universal symbolism we have developed [12], taking into account (1), we can write the equation of a moment of arbitrary order:

$$\frac{\partial \mathbf{M}_e^{[k]}}{\partial t} + \nabla \cdot \mathbf{M}_e^{[k+1]} + k \frac{e}{m_e} \left\lfloor \mathbf{M}_e^{[k-1]} \vec{E} + \mathbf{M}_e^{[k]} \times \vec{B} \right\rfloor = \frac{\delta \mathbf{M}_e^{[k]}}{\delta t}, \qquad (8)$$

where

$$\frac{\delta \mathbf{M}_e^{[k]}}{\delta t} = m_e \int \frac{\delta f_e(\vec{v})}{\delta t} \vec{v}^{\lceil k \rceil} d\vec{v}. \qquad (9)$$

Equation (9) is the continuity equation (for $k = 0$), the motion equation (at $k = 1$), the momentum flux equation (at $k = 2$), half of the trace of all terms in which is the energy equation.

The main problem in EGD (as in gas dynamics in general) is the fundamental non-closure of the equations system. The second term of the kinetic equation (1) in each equation (8) of the new order k creates a second term not represented in the equations of previous orders. In "classical" gas dynamics, approximate closure of the system is achieved using the Maxwell distribution of electron velocity within the framework of the LTE method, which, as already mentioned, is applicable only to relatively dense gases.

In the absence of maxwellization factors (intense collisions), in EPD with closed electron drift there are isotropy factors in the electron velocity distribution [11], which allows the application of CKFM, limiting itself in (7) to integration only over the total solid angle:

$$\mathbf{F}^{[k]}(t, \vec{r}, v) = \frac{1}{4\pi} \int\limits_\Omega f_e(t, \vec{r}, \vec{v})\, i_v^{\lceil k \rceil} d\Omega, \qquad (10)$$

where $\mathbf{F}^{[k]}$ – angular momentum of the distribution function; i_v – unit velocity vector.

The transition to gas-dynamic parameters (7) is determined by the expression:

$$\mathbf{M}_e^{[k]}(t, \vec{r}) = 4\pi m_e \int\limits_0^\infty \mathbf{F}^{[k]}(t, \vec{r}, v) v^{k+2} dv. \qquad (11)$$

Within the framework of CKFM, one can write the equation of angular moment of arbitrary order:

$$\frac{\partial \mathbf{F}^{[k]}}{\partial t} + v\nabla \cdot \mathbf{F}^{[k+1]} + k\frac{e}{m_e}\left\lfloor \mathbf{F}^{[k]} \times \vec{B} \right\rfloor -$$
$$-\frac{e}{m_e v}\left(\vec{E} \cdot \frac{1}{v^{k+1}} \frac{\partial}{\partial v}\left(v^{k+2} \mathbf{F}^{[k+1]} \right) - \right. , \quad (12)$$
$$\left. -k\left\lfloor \mathbf{F}^{[k-1]} \vec{E} \right\rfloor \right) = \frac{\delta \mathbf{F}^{[k]}}{\delta t}$$

where $\lfloor ...... \rfloor$ – symmetry operation [11]; $\frac{\delta \mathbf{F}^{[k]}}{\delta t}$ – angular collision integral:

$$\frac{\delta \mathbf{F}^{[k]}(v)}{\delta t} = \frac{1}{4\pi}\int \frac{\delta f_e(\vec{v})}{\delta t} i_v^{[k]}(\vec{v}) d\Omega . \quad (13)$$

It can be noted that, being similar to the moment equation (8), expression (12) retains in the first term in brackets in the second line the feature of the kinetic equation (1).

2.2. Average values of the volume coefficient and ionization cross-section

The main factors of non-equilibrium that determine the difference between the electron distribution function and the Maxwell one are:

- dissipative flow of electron energy beyond the plasma boundaries through the potential barrier in the bipolar boundary layer [13];
- dissipative flow of electron momentum from the plasma due to non-mirror reflection of electrons from the potential barrier [13];
- loss of electron energy in acts of impact ionization in the volume [14].

Just as in gas dynamics, the system of angular moments equations CKFM is fundamentally not closed, and can be closed approximately.

Using equation (12) and materials presented in papers [14], calculations were made of the electron velocity distribution function and the characteristics of the boundary bipolar layer in the Hall thruster [13].

The main characteristic of ionization in the continuity and energy equations is the so-called volume ionization coefficient β_i:

$$\beta_i = \langle v_e \sigma_i \rangle = \int_{e\varphi_i}^{\infty} f(\varepsilon) v(\varepsilon) \sigma_i(\varepsilon) \sqrt{\varepsilon}\, d\varepsilon , \quad (14)$$

where $m_e v^2(\varepsilon) = 2\varepsilon$ – energy of the primary electron; $f(\varepsilon) = 4\pi F^{(0)}(v(\varepsilon))$ – angular momentum of the distribution function (10) of the 0th order.

Average ionization cross-section according to (14):

$$\tilde{\sigma}_i = \frac{\beta_i}{\langle v_e \rangle} = \frac{\int_{e\varphi_i}^{\infty} f(\varepsilon) v(\varepsilon) \sigma_i(\varepsilon) \sqrt{\varepsilon}\, d\varepsilon}{\int_0^{\infty} f(\varepsilon) v(\varepsilon) \sqrt{\varepsilon}\, d\varepsilon} . \quad (15)$$

Dependence of the ionization cross-section on the energy of the primary electron in accordance with the modified Thomson formula [14]:

$$\sigma_i(\varepsilon) = \sigma_{i\,max} \frac{\left(1+\sqrt{3}\right)^2 e\varphi_i (\varepsilon - e\varphi_i)}{\varepsilon(\varepsilon + 2e\varphi_i)} , \quad (16)$$

where $\sigma_{i\,max}$ – maximum value σ_i.

Expression (15) in dimensionless variables has the form:

$$\tilde{\sigma}_i = \left(1+\sqrt{3}\right)^2 \sigma_{i\,max} \frac{\psi_i \int_{\psi_i}^{\infty} f(z) \frac{z-\psi_i}{z+2\psi_i} dz}{\int_0^{\infty} f(z) z\, dz} \quad (17)$$

or

$$\tilde{\sigma}_i = \left(1+\sqrt{3}\right)^2 \sigma_{i\,max} \frac{\psi_i \int_0^{\infty} f(z+\psi_i) \frac{z}{z+3\psi_i} dz}{\int_0^{\infty} f(z) z\, dz} \quad (18)$$

where

$$z = \frac{\varepsilon}{kT_e} , \qquad \psi_i = \frac{e\varphi_i}{kT_e} . \quad (19)$$

Introducing $f(z)$ as

$$f(z) = f(0) e^{-u(z)} , \quad (20)$$

it can be written:

$$\tilde{\sigma}_i = \left(1+\sqrt{3}\right)^2 \sigma_{i\,max} \frac{\psi_i \int_0^{\infty} e^{-u(z+\psi_i)} \frac{z}{z+3\psi_i} dz}{\int_0^{\infty} e^{-u(z)} z\, dz} . \quad (21)$$

For the Maxwell distribution:

$$u(z) = z . \quad (22)$$

When calculating in accordance with

ISSN 1727-7337 (print)
ISSN 2663-2217 (online)

expression (21), it is convenient to identify the factors:

- energy spectrum of electrons (Fig. 1):

$$e^{\Psi(\psi_i)} = \frac{\int_0^\infty e^{-u(z+\psi_i)} z\,dz}{\int_0^\infty e^{-u(z)} z\,dz}; \qquad (23)$$

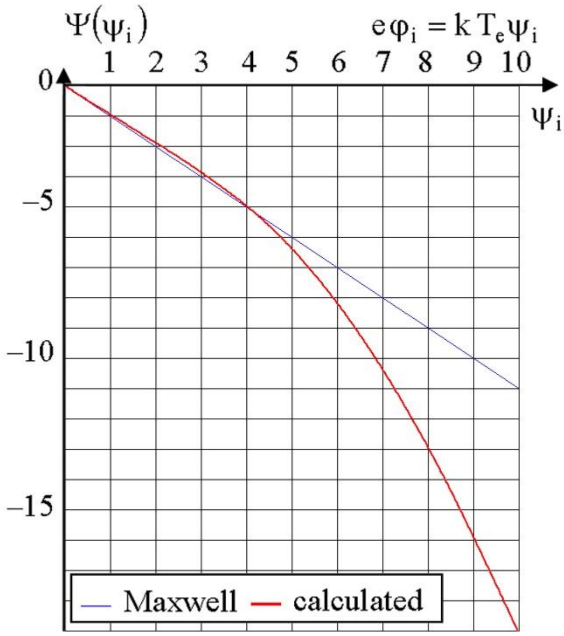

Fig. 1. Function $\Psi(\psi_i)$

- dependence of the ionization cross-section on the energy of the primary electron (Fig. 2):

$$R(\psi_i) = \frac{\left(1+\sqrt{3}\right)^2 \psi_i \int_0^\infty e^{-u(z+\psi_i)} \frac{z}{z+3\psi_i} dz}{\int_0^\infty e^{-u(z+\psi_i)} z\,dz}. \qquad (24)$$

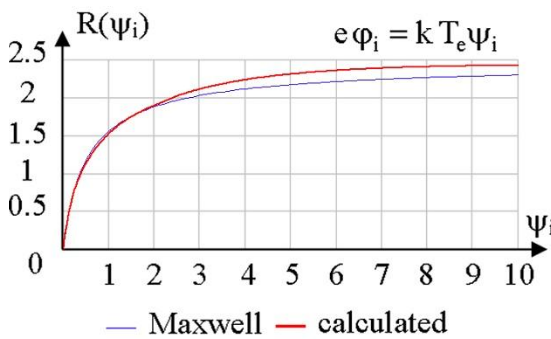

Fig. 2. Function $R(\psi_i)$

In this case:

$$\tilde{\sigma}_i = \sigma_{i\max} e^{-\psi_i} S_i(\psi_i), \qquad (25)$$

where (Fig. 3)

$$S_i(\psi_i) = e^{\Psi(\psi_i)+\psi_i} R(\psi_i), \qquad (26)$$

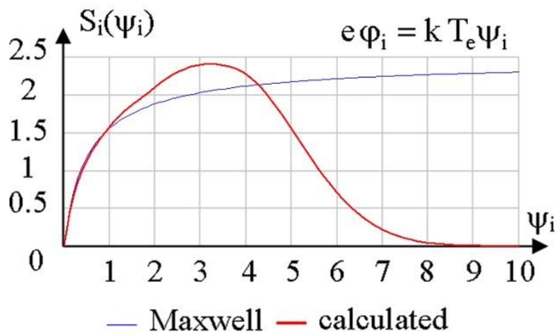

Fig. 3. Function $S_i(\psi_i)$

For the Maxwell distribution:

$$\Psi_M(\psi_i) = -\psi_i. \qquad (27)$$

$$S_{iM}(\psi_i) = R_M(\psi_i) = = \left(1+\sqrt{3}\right)^2 \psi_i \int_0^\infty e^{-z} \frac{z}{z+3\psi_i} dz. \qquad (28)$$

Dependence $\Psi(\psi_i)$ with absolute error $\Delta\Psi \le 0.01$ can be represented by an approximation (Table 1):

$$\Psi(\psi_i) = a_0 + a_1\psi_i + a_2\psi_i^2. \qquad (29)$$

Table 1

Approximation coefficients (29)

ψ_i	a_0	a_1	a_2
<0.2	0	1.125	0
0.2 – 1.8	0.0414	0.9163	0.0094
1.8 – 3.8	0.3576	0.6411	0.0665
3.8 – 8.6	2.1572	-0.3121	0.1927
8.6 – 10	-7.1659	1.7996	0.0732
>10	-14.048	3.2200	0

Dependence $R(\psi_i)$ with relative error $\delta R \le 0.0025$ can be represented by an approximation (Table 2):

$$R(\psi_i) = \frac{7.4641\psi_i}{a_0 + (a_1 + a_2\psi_i)\psi_i}. \qquad (30)$$

Table 2

Approximation coefficients (30)

ψ_i	a_0	a_1	a_2
0 – 1	1.37	3.98	–0.49
1 – 2	1.90	2.92	0.04
2 – 10	3.26	1.88	0.20
>10	0.62	3.00	0

2.3. Analysis of the interdependence of ionization processes and the formation of electron energy distribution

It can be seen (Fig. 3) that the calculated value of $\tilde{\sigma}_i$ is significantly inferior to that found for the Maxwell distribution in the electron temperature region, starting at a value five times lower than the ionization potential. In this region, ionization is produced by electrons whose energy is sufficient to overcome the potential barrier in the boundary layer.

Fig. 4, Fig. 5 show a comparison of the electron energy distribution function in a Hall thruster on xenon, calculated in work [13], with the Maxwell one at $e\varphi_i = 5kT_e$, where φ_i – ionization potential. The height of the potential barrier in this case $e\Delta\varphi = 4.910kT_e$.

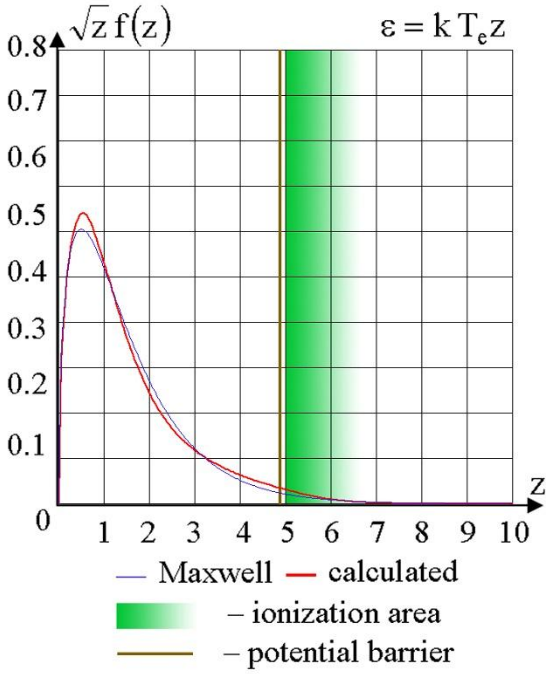

$kT_e = 0.2e\varphi_i$ $\quad$ $e\Delta\varphi = 4.910kT_e$

Fig. 4. Electron energy distribution function

One can notice a deficit of electrons in the ionization region due to their intensive escape from the plasma. Somewhat unexpectedly, the value turned out to be greater than for the Maxwell distribution $\tilde{\sigma}_i$ in the high energy region (Fig. 3). Fig. 6, Fig. 7 shows a comparison of the electron energy distribution function calculated in [13] with the Maxwell on at $e\varphi_i = 0.25kT_e$. The height of the potential barrier in this case $e\Delta\varphi = 5.060kT_e$.

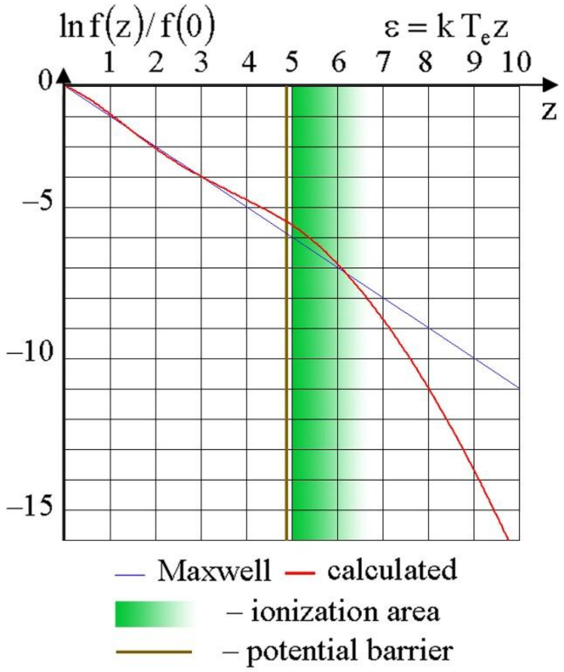

$kT_e = 0.2e\varphi_i$ $\quad$ $e\Delta\varphi = 4.910kT_e$

Fig. 5. Electron energy distribution function

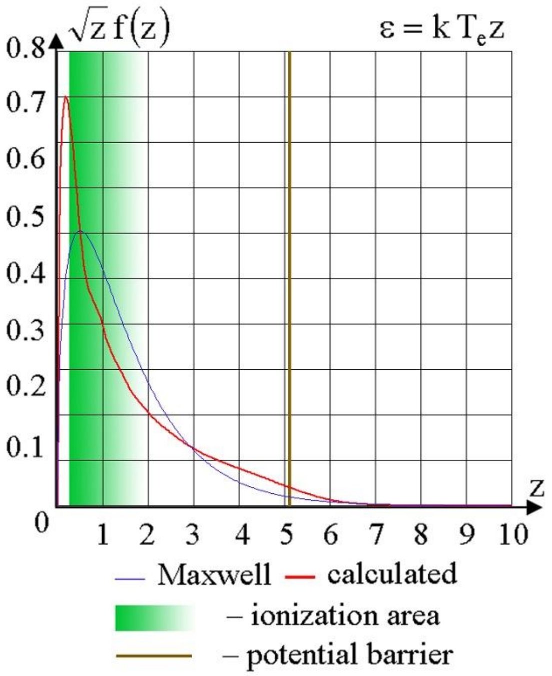

$kT_e = 4e\varphi_i$ $\quad$ $e\Delta\varphi = 5.060kT_e$

Fig. 6. Electron energy distribution function

 ISSN 1727-7337 (print)
ISSN 2663-2217 (online)

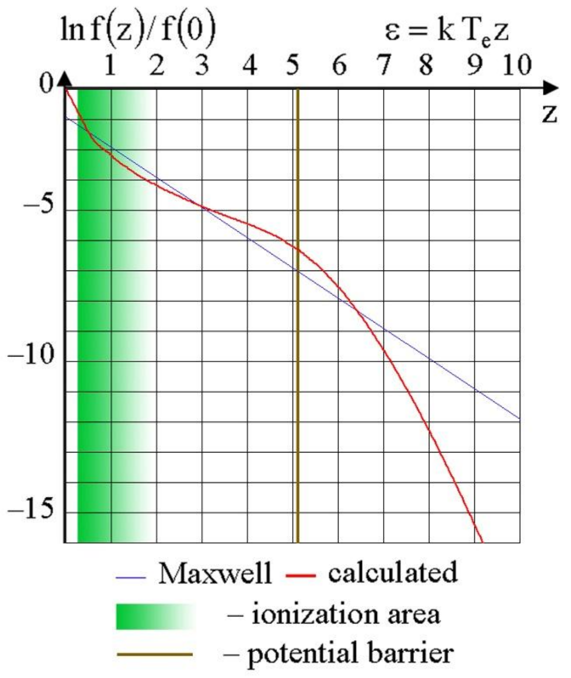

$k\,T_e = 4\,e\,\varphi_i$ $\qquad$ $e\,\Delta\varphi = 5.060\,k\,T_e$

Fig. 7. Electron energy distribution function

Here it can be seen an excess of electrons in the region of intense ionization and, mainly - lower.

3. Results and Discussion

Thus, it can be assumed that there is a direct and feedback relationship between the processes of ionization and the formation of electron energy distribution.

The expression for the angular integral of ionization collisions found in [14] can be represented as:

$$\frac{\delta_i f_0(v)}{\delta t} = \frac{\delta_i^{+} f_0(v)}{\delta t} - \frac{\delta_i^{-} f_0(v)}{\delta t}, \qquad (31)$$

where the first term on the right side corresponds to the arrival of secondary electrons in the region of lower energies, and the second to the departure of primary electrons from the region of higher energies.

It can be written:

$$\frac{\delta_i^{\pm} f_0(v)}{\delta t} = n_a \sigma_{im} \frac{2\,e\,\varphi_i}{m_e v} f_0(v) I_i^{\pm}\left(\frac{e\,\varphi_i}{k\,T_e}, \frac{m_e v^2}{2\,k\,T_e}\right), \qquad (32)$$

where n_a – population of atoms; σ_{im} – maximum of dependence of the ionization cross-section on energy.

In this case:

$$I_i^{-}(\psi_i, z) = \max\left(\frac{z - \psi_i}{z + 2\,\psi_i}, 0\right), \qquad (33)$$

$$I_i^{+}(\psi_i, z) = \frac{12\,z}{f_0(z)} \int_z^{\infty} f_0(z' + \psi_i) \frac{z' - z}{z' + 3\,\psi_i} \frac{d\,z'}{z'^2}. \qquad (34)$$

The regions of predominant incoming or outgoing electrons are highlighted In Fig. 8.

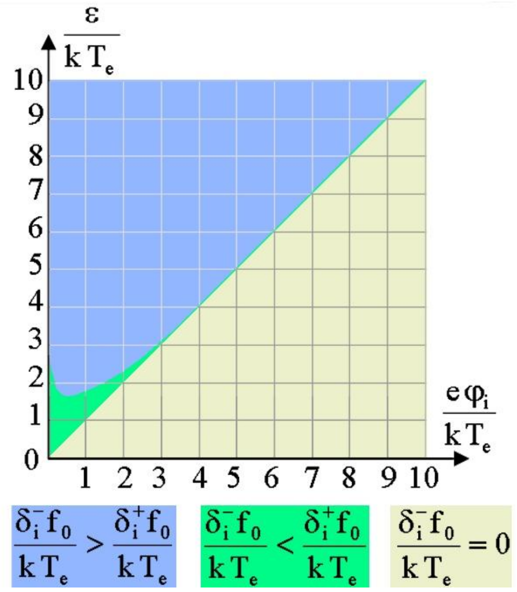

Fig. 8. Regions of predominant incoming or outgoing electrons

For example, the value $e\,\varphi_i = 5\,k\,T_e$ (Fig. 4, Fig. 5) corresponds to a sharp transition from the region $\frac{\delta_i^{-} f_0(v)}{\delta t} > \frac{\delta_i^{+} f_0(v)}{\delta t}$ to the region $\frac{\delta_i^{-} f_0(v)}{\delta t} = 0$ and relatively uniform filling of the electron energy region $\varepsilon < e\,\varphi_i$ with the distribution of their energy in this region close to Maxwell's:

$$f_0 + k\,T_e \frac{\partial f_0}{\partial \varepsilon} \approx 0. \qquad (35)$$

On the contrary, the meaning $e\,\varphi_i = 0.25\,k\,T_e$ (Fig. 6, Fig. 7) corresponds to the presence of an extended region $0 < \frac{\delta_i^{-} f_0(v)}{\delta t} < \frac{\delta_i^{+} f_0(v)}{\delta t}$ with the distribution function of their energy in this region exceeding the Maxwell one, but with

$$f_0 + k\,T_e \frac{\partial f_0}{\partial \varepsilon} < 0. \qquad (36)$$

A positive value on the left-hand sides of (35) and (36) in elastic electron-atom, electron-ion, and electron-electron collisions generally means a "top-down" electron flow in energy space, while a negative value, as in (36), means a "bottom-up" flow. However, in a rarefied EPD plasma, the intensity of these collisions is clearly insufficient to form an electron distribution close to Maxwell. The effect of an electromagnetic field may be a factor in this closeness.

The distributions presented in Fig. 4 – Fig. 7 were found in the work [13] as a result of solving the equations of the M1+ angular model, that is, by writing equation (12) for the zero and first angular moments:

$$\frac{\partial f_0}{\partial t}+v\nabla\cdot\vec{f}_1-\frac{e}{m_e v}\vec{E}\cdot\frac{1}{v}\frac{\partial}{\partial v}\left(v^2\vec{f}_1\right)=\frac{\delta f_0}{\delta t}, \quad (37)$$

$$\frac{\partial\vec{f}_1}{\partial t}+v\nabla\cdot\mathbf{F}^{[2]}+\frac{e}{m_e}\vec{f}_1\times\vec{B}-\frac{e}{m_e v}\left(\vec{E}\cdot\frac{1}{v^2}\frac{\partial}{\partial v}\left(v^3\mathbf{F}^{[2]}\right)-\vec{E}f_0\right)=\frac{\delta\vec{f}_1}{\delta t}, \quad (38)$$

where $f_0=\mathbf{F}^{[0]}$, $\vec{f}_1=\mathbf{F}^{[1]}$ – spherical functions of 0th and 1st order [11, 12].

According to (10) it can be seen that the trace of angular moment $\mathbf{F}^{[k]}$ at $k>1$ contains the previous moments of the same parity $\mathrm{Tr}\,\mathbf{F}^{[k]}=\mathbf{F}^{[k-2]}$.

Spherical functions constructed as linear combinations of angular moments contain only new information at a new degree of anisotropy $\mathrm{Tr}\,\mathbf{f}^{[k]}=0$.

In this case:

$$\mathbf{F}^{[2]}=\frac{1}{3}\boldsymbol{\delta}f_0+\frac{2}{3}\mathbf{f}^{[2]}. \quad (39)$$

In case of transverse $\vec{E}=i_E E$ and $\vec{B}=i_B B$ at $i_\perp=i_E\times i_B$ it can be written:

$$\vec{f}_1=i_E f_E+i_B f_B+i_\perp f_\perp, \quad (40)$$

where, under closed-drift EPD conditions, the drift projection of the electron flux density is dominant $f_\perp$.

Accordingly, the prevailing in $\mathbf{f}^{[2]}$ is the component corresponding to the viscous flow of the Hall projection of the electron momentum along the magnetic lines:

$$\mathbf{f}^{[2]}=\left(i_B i_\perp+i_\perp i_B\right)f^{(\perp B)}. \quad (41)$$

Assuming that the distribution of electrons in space is close to the Boltzmann distribution:

$$\nabla f_0=-\frac{e\vec{E}}{kT_e}f_0 \quad (42)$$

expressions (37), (38) can be written in the form:

$$\nabla\cdot\vec{\Gamma}_r+\frac{1}{v^2}\frac{\partial}{\partial v}\left(v^2\Gamma_v\right)=\frac{\delta_i f_0}{\delta t}, \quad (43)$$

$$\frac{1}{3}v\frac{eE}{kT_e}\left(f_0+\frac{kT_e}{m_e}\frac{1}{v}\frac{\partial f_0}{\partial v}\right)+\frac{eB}{m_e}f_\perp=\frac{v}{\lambda_V}f_E, \quad (44)$$

$$\frac{2}{3}v\frac{\partial f^{(\perp B)}}{\partial x_B}+\frac{eB}{m_e}f_E=-\frac{v}{\lambda_V}f_\perp, \quad (45)$$

where x_B – coordinate along the magnetic line; λ_V – the relaxation length of the electron momentum in collisions in the volume; $\vec{\Gamma}_r$ and Γ_v – electron flux density in the space of coordinates and velocity modulus:

$$\vec{\Gamma}_r=v\vec{f}_1, \qquad \Gamma_v=-\frac{eE}{m_e}f_E. \quad (46)$$

An approximate closure of system (43)–(45) can be achieved using the results of [15]:

$$\frac{\partial f^{(\perp B)}}{\partial x_B}=\frac{\eta_p}{X_B}f_\perp, \quad (47)$$

where X_B – the size of the device channel in the direction of the magnetic line; η_p – the relaxation coefficient of electron momentum in the bipolar boundary layer.

In this case, from (45), (46) we have:

$$\frac{eB}{m_e}f_E=-\frac{1}{\lambda_\Sigma}vf_\perp, \quad (48)$$

$$\Gamma_v=-w_{EB}\frac{m_e v^2}{3kT_e}\left(f_0+\frac{kT_e}{m_e v}\frac{\partial f_0}{\partial v}\right), \quad (49)$$

where

$$\frac{1}{\lambda_\Sigma}=\frac{1}{\lambda_V}+\frac{2}{3}\frac{\eta_p}{X_B}, \quad (50)$$

$$w_{EB}=\frac{\left(\frac{eE}{m_e}\right)^2}{\frac{v^2}{\lambda_V}+\lambda_\Sigma\left(\frac{eB}{m_e}\right)^2}. \quad (51)$$

That is, as in elastic collisions in the volume, the action of the electromagnetic field means a flow of

 ISSN 1727-7337 (print)
ISSN 2663-2217 (online)

electrons in the energy space (velocity modulus) “from bottom to top” in case (36) and vice versa in the opposite case.

It is characteristic thus, that the directions of electrons flows in energy space are identical in an accelerating and decelerating electric field and depend only on the sign in brackets of expression (49).

4. Conclusions

In accordance with the stated objective of the study, the following tasks were solved:

1. The analysis of the sequence "kinetics – EGD – CKFM" was carried out taking into account the impact ionization process.

2. An expression is written for the average values of the volume coefficient and ionization cross-section over the electron energy spectrum.

3. An analysis of the behavior of the calculated values revealed the interdependence of ionization processes and the formation of the electron energy spectrum. The electron flux from the energy region where ionization-induced electron influx predominates results in an excess of electrons in this region compared to the Maxwell distribution. This excess, in turn, increases the average cross-section and impact ionization rate at high electron temperatures.

The prospect of further research involves generalizing the obtained results to the process conditions in different types of EPD operating on different working fluids.

Conflict of Interest

The author declares that he has no conflict of interest in relation to this research, whether financial, personal, author ship or otherwise, that could affect the research and its results presented in this paper.

Financing

This research was conducted without financial support.

Data Availability

The manuscript has no associated data.

Use of Artificial Intelligence

The author confirms that he did not use artificial intelligence technologies when creating the current work.

Acknowledgments

The author expresses gratitude to Serhii Nesterenko, Associate Professor of the Department of Space Engineering and Renewable Power Sources of the National Aerospace University "Kharkiv Aviation Institute", for assistance in the mathematical analysis of the processes that are the subject of the study.

The author has read and agreed to the published version of this manuscript.

References

1. Pitaevskii, L. P. Physical Kinetics, Volume 10. *Butterworth-Heinemann*, 1981. 464 p.

2. Fitzpatrick, R. Courses Taught By Richard Fitzpatrick at University of Texas at Austin. Available et: https://farside.ph.utexas.edu/teaching.html

3. Fife, J. M. Hybrid-PIC Modeling and Electrostatic Probe Survey of Hall Thrusters : PhD thesis. *Massachusetts Institute of Technology, Department of Aeronautics*, 1998. 256 p.

4. Ortega, A. L., Mikellides, I. G. 2D Fluid-PIC Simulations of Hall Thrusters with Self-Consistent Resolution of the Space-Charge Regions. *Plasma*, 2023, vol. 6, iss. 3, pp. 550-562. DOI: 10.3390/plasma6030038.

5. Hofer, R. R., Katz, I., Mikellides, I., Gamero-Castano, M. Heavy Particle Velocity and Electron Mobility Modeling in Hybrid-PIC Hall Thruster Simulations. *The 42nd AIAA/ASME/SAE/ASEE Joint Propulsion Conference & Exhibit*, 2006. 17 p. DOI: 10.2514/6.2006-4658.

6. Panelli, M., Morfei, D., Milo, B., D’Aniello, F. A., Battista, F. Axisymmetric Hybrid Plasma Model for Hall Effect Thrusters. *Particles*, 2021, no 4, iss 2, pp. 296-324. DOI: 10.3390/particles4020026

7. Guisset, S., Brull, S., Dubroca, B., d’Humières, E., Karpov, S., Potapenko, I. Asymptotic-preserving scheme for the Fokker-Planck-Landau-Maxwell system in the quasi-neutral regime. *Communications in Computational Physics*, 2016, vol. 19, iss. 02, pp. 301-328.

8. Guisset, S., Aregba, D., Brull, S., Dubroca, B. The M_1 angular moments model in a velocity-adaptive frame for rarefied gas dynamics applications. *Multiscale Modeling & Simulation*, 2017, vol. 15, iss. 4. 30 p.

9. Guisset, S. Angular moments models for rarefied gas dynamics. Numerical comparisons with kinetic and Navier-Stokes equations. *Kinetic and Related Models (KRM)*, 2020, vol. 13, iss. 4, pp. 739-758. DOI: 10.3934/krm.2020025

10. Guisset, S., Brull, S., d’Humières, E., Dubroca, B., Tikhonchuk, V. Classical transport theory for the collisional electronic M1 model. Physica A: Statistical Mechanics and its Applications, 2016, vol. 446. 19 p.

11. Nesterenko, S., Zhihao, H., Roshanpour, S. Compromise kinetic-fluid model of electrons dynamics

in electric propulsion devices with closed electrons drift as an alternative to the hybrid PIC-Fluid method. *Aerospace Technic and Technology*, 2025, no. 1 (201), pp. 28-37. DOI: 10.32620/aktt.2025.1.03

12. Nesterenko, S., Huang Zhihao, Roshanpour, S. Mathematical aspects of M-unlimited angular model in electric propulsion. *The 2nd International scientific and practical conference "Challenges and Opportunities in Modern Scientific Research"*, 2025, iss. 16, pp. 208-213.

13. Nesterenko, S., Huang, Z., Roshanpour, S. Parameters of the bipolar boundary layer in electric propulsion thrusters with closed electron drift: M1+ angular model. *The 2nd International scientific and practical conference "Modern Scientific Research: Theoretical and Practical Aspects"*, 2025, iss 37, pp. 462-479.

14. Guo, Z., Huang, Z., Peng, S. The role of impact ionization in the balance of particles, momentum and energy in plasma-ion and Hall effect thrusters. *The XXXI International Scientific and Practical Conference "Trends in the development of modern scientific"*, Vancouver, Canada, 2021, pp. 399-440.

15. Loyan, A. V., Nesterenko, S. Yu., Guo Z., Huang Z. Quasi-one-dimensional mathematical model of processes in Hall effect and plasma-ion thrusters. *Open Information and Computer Integrated Technologies*, 2021, no 92, pp. 41-54.

Received 15.07.2026, Received in revised form 29.07.2026
Accepted date 17.08.2026, Published date 26.08.2026

АНАЛІЗ ВЗАЄМОЗАЛЕЖНОСТІ ПРОЦЕСІВ ІОНІЗАЦІЇ ТА ФОРМУВАННЯ РОЗПОДІЛУ ЕНЕРГІЇ ЕЛЕКТРОНІВ У ЕЛЕКТРОРАКЕТНИХ ПРИСТРОЯХ

Шахрам Рошанпур

Об'єктом даного дослідження є процеси у нерівноважній плазмі електроракетних пристроїв. **Предметом** дослідження є ударна іонізація з урахуванням її зворотного зв'язку з енергетичним спектром електронів. **Метою** дослідження є відшукання виразів для показників ударної іонізації у правих частинах рівнянь математичної моделі процесів в електроракетних пристроях з урахуванням компромісної kinetic-fluid моделі. **Завдання**: проаналізувати існуючі різновиди механіки суцільного середовища з урахуванням процесу ударної іонізації з використанням результатів, представлених у попередніх роботах автора; записати вираз для середніх за енергетичним спектром електронів величин об'ємного коефіцієнта та перерізу іонізації, проаналізувати поведінку розрахованих величин з урахуванням взаємозалежності процесів іонізації та формування розподілу енергії електронів. **Методи**, використані у дослідженні, включають аналітичне дослідження існуючих моделей процесів з визначенням меж їх застосування у розрідженій плазмі; теоретичний аналіз ролі ударної іонізації у формуванні енергетичного спектру електронів з урахуванням особливостей плазми, обмеженої потенційними бар’єрами у пограничному біполярному прошарку. Обчислені залежності в області енергій вище за потенційний бар'єр показали значення нижчі у порівнянні зі знайденими при максвеллівському розподілі, але вищі в області нижче за потенціал іонізації при великих температурах електронів. На основі аналізу впливу енергетичного спектру електронів на інтенсивність іонізації та впливу електромагнітного поля на транспортування електронів у просторі енергії було показано додатний зворотний зв'язок: при відносно високих температурах електронів необхідність їх транспортування "вгору" з області нижче потенціалу іонізації призводить до їх надлишку в цій області; у свою чергу цей надлишок призводить до збільшення середнього за енергією перерізу іонізації і збільшення їх надлишку у нижній частині спектра.

Ключові слова: електроракетні пристрої, розподіл енергії електронів; ударна іонізація; потенційний бар'єр; біполярний прикордонний прошарок; модель кутових моментів.

Шахрам Рошанпур – Інженер-дослідник, IL Sentiero International Campus, Schio VI, Італія.

Shahram Roshanpour – Engineer/Researcher, IL Sentiero International Campus, Schio VI, Italy.
e-mail: space.science@protonmail.com, ORCID: 0000-0002-4272-9217, Scopus Author ID: 60693707500.